

# Cross-Network Performance Analysis of Network Coding Aided Cooperative Outband D2D Communications

Eftychia Datsika, *Student Member, IEEE*, Angelos Antonopoulos, *Senior Member, IEEE*, Nizar Zorba, *Member, IEEE*, Christos Verikoukis, *Senior Member, IEEE*

**Abstract**—In Long Term Evolution Advanced (LTE-A) networks, the mobile devices can concurrently participate in cooperative outband Device-to-Device (D2D) data exchange by virtue of user- or network-related parameters (e.g., interest in the same content and cooperative transmissions, respectively). In these scenarios, two major problems arise: i) the coexistence of multiple devices creates channel access issues, demanding effective Medium Access Control (MAC) schemes, and ii) cellular network factors (i.e., scheduling policy and channel conditions) affect the D2D communication, as the circulating information in D2D links is mainly of cellular network origination, stressing the need for cross-network approaches. In this context, the contribution of this paper is threefold. First, exploiting idle devices as relays and the benefits of Network Coding (NC) in bidirectional communications, we propose an Adaptive Cooperative NC-based MAC (ACNC-MAC) protocol for D2D data exchange. Then, we devise a cross-network model that captures the impact of cellular network characteristics on D2D communication. Finally, we evaluate the performance of ACNC-MAC in terms of throughput, energy efficiency and battery consumption. Our results show that LTE-A parameters and the relays' participation significantly affect the D2D throughput, while the D2D performance deteriorates with the increase of cell congestion.

**Index Terms**—D2D Communication, LTE-A Networks, Cooperation, Network Coding, MAC Protocols.

## I. INTRODUCTION

MOBILE data traffic worldwide will increase tenfold by the year 2019, with smartphones accounting for three quarters of the total traffic [1]. The launch of Long Term Evolution Advanced (LTE-A) networks and the outstanding proliferation of smart mobile devices offer the users an unprecedented variety of multimedia services [2]. Future mobile broadband systems have to accommodate an increasing number of always connected users of various mobile applications, e.g., video streaming, content sharing, online games and social networking services. The requirement for ubiquitous wireless access and delivery of high Quality of Service (QoS) are main challenges for the development of LTE-A networks [3].

A tremendous amount of data is exchanged between network components, e.g., LTE-A evolved NodeB base stations

(eNBs) and user equipment terminals (UEs). As cellular networks become denser, due to the ever-growing number of UEs using data intensive applications, the efficient radio resource management becomes crucial. A promising technology that can alleviate cell congestion is Device-to-Device (D2D) communication that enables direct communication among UEs without the eNB's intervention [4]. Although the 3rd Generation Partnership Project (3GPP) specification defines D2D communication as a means for communication recovery in public safety use cases [5], the D2D concept has been investigated in academia as a traffic offloading solution [6]. It is also considered as an offloading solution by leader telecommunications companies, e.g., Nokia [7]. With the emergence of new wireless standards, like Wi-Fi Direct [8] and Millimeter-wave communication [9], which enable UEs' direct connectivity, the integration of D2D communication into cellular networks seems appealing. In hybrid cellular/D2D networks, the eNBs can take advantage of UEs' proximity and establish D2D links, in order to increase the spectral efficiency [10]. D2D connections can operate in licensed frequency band along with cellular communication links, being under cellular control (*inband D2D*), or in unlicensed spectrum (*outband D2D*) [11].

## A. Motivation

Main advantages of outband D2D communication are the unbinding of cellular system resources and the absence of interference from D2D connections to eNB-UE communication. Several works advocate for the use of D2D communication as a way to mitigate the limited network capacity problem. Resource allocation can be performed using D2D clustering techniques and Wi-Fi Direct, combined with inter-cell interference control methods [12]. UE cluster formation can be a scheduling scheme, where only the cluster head receives data from the eNB and forwards them to the rest of the UEs [13]. However, the organization of clusters cannot easily adapt to volatile distributed topologies, and the assignment of the cluster head role to a particular UE, e.g., the one with the highest channel quality, is not fair especially regarding the energy consumption. The outband D2D can reduce the eNB-UE communication overhead, as downlink traffic can be offloaded to D2D connections, when UEs are in proximity. However, existing offloading techniques, e.g., [14], do not consider the outband D2D channel access issues.

The UEs' close proximity and the D2D data dissemination over Wi-Fi links create opportunities for UE cooperation. The

This work has been funded by the Research Projects AGAUR (2014-SGR-1551) and CellFive (TEC2014-60130-P).

E. Datsika is with IQUADRAT Informatica S. L., Barcelona, Spain. E-mail: edatsika@iquadrat.com.

A. Antonopoulos and C. Verikoukis are with Telecommunications Technological Center of Catalonia (CTTC/CERCA), Castelldefels, Spain. E-mail: {aantonopoulos, cveri}@cttc.es.

N. Zorba is with Qatar University, Doha, Qatar. E-mail: nizarz@qu.edu.qa.

formation of D2D networks can be an initiative either from the UEs or the cellular network. From the user's perspective, the coexistence of UEs that express their interest in downloading similar digital content from the eNB, e.g., video clips and advertisements, is typical in social activities, e.g., concerts or sports events [15]. Multiple neighboring UEs might desire to share multimedia content downloaded from eNB and create D2D clusters. UE cooperation helps circumventing transmissions from eNB to each UE separately, as devices can exchange data portions via Wi-Fi [16]. The UEs can share downloaded content fractions with peers via D2D bidirectional flows. Likewise, bidirectional D2D data dissemination can be performed by location-aware applications or multimedia services requiring information exchange between UE pairs, e.g., video telephony. Besides being useful in user-oriented scenarios, D2D cooperation can be a solution to poor D2D link quality problems. From the network's perspective, device collaboration can be facilitated by the exploitation of UEs as relays, when devices willing to communicate experience bad channel conditions. The UEs' participation in collaborative clusters can be rewarded by mobile network operators, making the cooperative transmission beneficial for both UEs requesting content and their helpers [17]. For instance, idle UEs with no interest in receiving specific content may be motivated to contribute as relays, if the operator provides incentives, e.g., lower service price or other types of remuneration [18].

Even though the internetworking between cellular and D2D connectivity is apparent in the aforementioned scenarios, it is an aspect often neglected by the outband D2D based schemes. In LTE-A, each eNB is responsible for the distribution of radio resources among the connected UEs, employing a variety of resource scheduling mechanisms. The utilized scheduling algorithm determines the achievable downlink data rates [19], which in turn regulate the packet arrival rates at UEs. As the resource allocation and transmission policies influence the frequency of packet arrivals, they further affect the QoS of D2D communication [20]. A joint methodology for user offloading to D2D network has been presented [21], which takes into account the interference among D2D links and captures the interaction between LTE-A and D2D connections. Despite its novel insights, this methodology does not consider the resource scheduling schemes and cellular data rates that cause differentiation in downlink performance among UEs.

In coexisting cellular and D2D networks, significant performance gains can be achieved by exploiting the devices' proximity, as UEs in the same area can act as relays and retransmit received and overheard packets. Conceptually, this store-and-forward process is related to the Network Coding (NC) technique, which allows intermediate nodes to combine data from the same or different information flows [22]. In D2D clusters formed by UEs connected through Wi-Fi links, the cooperation among devices can be leveraged by NC opportunities. The work published in [23] describes a scheme for data dissemination over D2D networks that exploits NC with the aim of improving the content availability at the UEs. This scheme regulates the data delivery considering the content correlation among neighboring UEs and utilizing the NC functionality for D2D data transmission. Nonetheless, it

does not consider the dissimilar downlink data rates stemming from different cellular link states for each UE, as well as Wi-Fi related problems arising during D2D transmissions, two factors that result in unequal QoS provision at UEs.

Despite the improvement of LTE-A spectral use realized by offloading traffic to D2D links, the network congestion may be inherited to D2D communication level. Wireless channel access issues appear in the Wi-Fi based D2D clusters due to simultaneous channel contention from multiple D2D users (UEs or relay nodes). In unlicensed bands, Wi-Fi is the prevalent wireless technology adopted for D2D connectivity and is based on the IEEE 802.11 standard. However, with the densification of D2D networks and the increasing random access attempts by UEs, the utilization of IEEE 802.11 standardized Medium Access Control (MAC) mechanism degrades the performance of cooperative transmissions. Furthermore, the time-varying quality of D2D links affects the throughput experienced by UEs, as the packet losses, caused by bad channel conditions, increase the number of packet retransmissions.

Under these circumstances, effective MAC mechanisms are required for the coordination of D2D communicating parties. NC has been widely utilized by MAC protocols, thanks to the throughput improvement it can achieve [24]. This inherent capability can be further exploited by access schemes that manage D2D cooperative retransmissions. So far, various NC-based MAC protocols have been presented. Making use of opportunistic listening and forwarding, the BEND protocol [25] combines packets at relay nodes, but requires broadcasting of the UEs' queue status information. The NCCARQ-MAC protocol [26] allows cooperation only when NC conditions are met and assumes that the sources are in saturated conditions. This is not always the case in realistic D2D networks where the packet arrival rates at UEs are determined by the LTE-A link performance. Using the Network Coding Aware Cooperative MAC protocol (NCAC-MAC) [27] for D2D cooperative communication would require strict synchronization among UEs, along with a physical layer protocol that can handle information retrieval from corrupted packets. For similar reasons, physical layer NC schemes are not straightforwardly applicable to D2D networking, because they demand coordination of simultaneous transmissions [28].

## B. Contribution and Structure of this Paper

In heterogeneous cellular/D2D networks, communication among UEs induces the use of different wireless technologies. The UEs can receive the desired data from the eNB, before sharing them through D2D links. The coexistence of different connection types entails cross-network interactions, thus the performance of D2D connections might be affected by the cellular network characteristics. Considering these challenges, this work brings the following contributions:

- (i) *Design of an efficient Adaptive Cooperative NC-based MAC protocol for the outband D2D communication (ACNC-MAC):* ACNC-MAC allows neighboring UEs to act as relays and perform cooperative transmissions, assisting the D2D communication of a UE pair. It goes beyond the state-of-the-art protocols, as it better exploits

NC opportunities arising in bidirectional D2D communication. The relays that overhear packets from both UEs can transmit encoded packets, serving both flows at each communication round. ACNC-MAC prioritizes the transmissions of relays that can perform NC, maximizing the benefits of the outband cooperative D2D communication.

- (ii) *Cross-network analysis of throughput performance of ACNC-MAC*: As the UEs that engage in D2D communication simultaneously receive the desired content from the eNB and share it with their peers, we study the D2D MAC performance in the LTE-A context. Particularly, the packet exchange rate at D2D level is dictated by the packet arrival rates at the UEs, which are affected by i) the downlink resource scheduling policy, and ii) the UEs' cellular downlink channel conditions. Considering these cross-network interactions between LTE-A and D2D communication levels, we propose the incorporation of cellular link parameters in the analysis of D2D MAC performance. Specifically, we present and validate an analytical model for the D2D throughput achieved by ACNC-MAC that captures the LTE-A parameters.
- (iii) *Evaluation of ACNC-MAC performance under the influence of concurrent cellular and D2D connectivity, simulating realistic scenarios*: We study the impact of LTE-A network characteristics (downlink transmission scheduling policies, downlink channel conditions and cell congestion levels) on D2D MAC performance and the ACNC-MAC behavior in the LTE-A context. Recognizing the escalating demand of digital video by mobile multimedia applications, we evaluate ACNC-MAC in D2D video transmission scenarios, where UEs exchange video content downloaded through cellular connections.

The remainder of the paper is organized as follows. The considered system model is described in Section II. In Section III, the ACNC-MAC protocol is presented, while the cross-network throughput analysis is provided in Section IV. Simulation results are discussed in Section V and, finally, in Section VI conclusions are drawn.

## II. SYSTEM MODEL

We consider a cellular network with one eNB and  $K$  UEs in the cell (Fig. 1). Each UE is equipped with two radio interfaces, LTE-A and Wi-Fi, thus being able to maintain connection to the eNB and simultaneously connect to other UEs via Wi-Fi. The UEs  $UE_1$  and  $UE_2$ , denoted as *active UE pair*, request content from eNB and establish LTE-A connections. Packets  $p$  and  $q$  arrive at  $UE_1$  and  $UE_2$ , respectively, through cellular connections. The two UEs are interested in each other's received content and they wish to establish bidirectional links among them. As this D2D network coexists with the cellular network, the D2D communication experiences challenges related to the interaction between LTE-A and Wi-Fi. Thus, we next describe the characteristics of both types of connections jointly considered in our work.

### A. LTE-A communication (eNB to UE)

The design of the LTE-A downlink physical layer is based on Orthogonal Frequency Division Multiplex Access

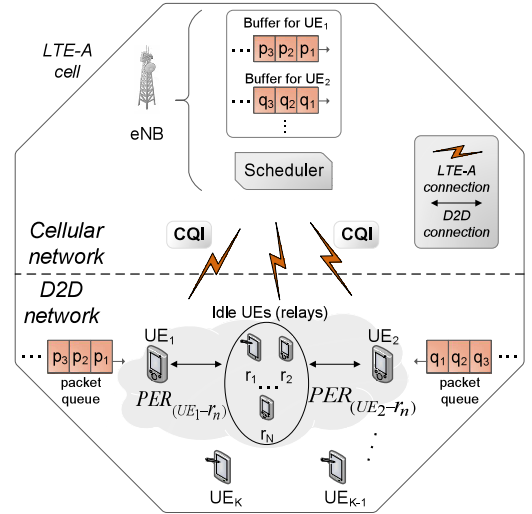


Fig. 1: D2D enabled LTE-A network

(OFDMA) scheme that allocates specific patterns of subcarriers in the time-frequency space to different users. The OFDM symbols required for the downlink transmissions are organized in  $N_{RB}$  Resource Blocks (RBs). A portion  $b$  of  $N_{RB}$  in the time-frequency domain is allocated to each UE by the eNB in every Transmission Time Interval (TTI).

1) *Downlink resource allocation*: Each UE's requirements regarding the allocated RBs stem from PHY layer parameters of eNB-UE connection that reflect the LTE-A link quality, i.e., the Signal-to-Noise Ratio (SNR) levels and the employed Modulation and Coding Schemes (MCSs). The resource sharing is managed by a scheduler entity at the eNB that has the role to assign RBs to the connected UEs. Various concepts for the LTE-A downlink scheduling algorithm exist [19], as no specific policy has been standardized. There are schedulers with different network performance targets, e.g., Round Robin, Maximum Throughput or Proportional Fair scheduler. The resulting data rate of each UE varies with respect to the selected scheduling policy. In our work, without loss of generality, we use a Round Robin scheduler that distributes evenly, in a TTI basis, the RBs among the active UEs, independently of the wireless channel conditions or QoS requirements.

2) *SNR estimation and MCS selection*: In the cell, the UEs are located in various distances from the eNB. We assume a fixed transmission power from the eNB. Thus, the UEs experience different SNR levels. The influence of the SNR heterogeneity is evident in the MCSs preferred for the downlink transmissions. The better the LTE-A link quality, the higher order MCS can be selected. In LTE-A, the MCS is determined according to Channel Quality Indicators (CQI) that depict each UE's downlink channel conditions and indicate the data rate supported by downlink channels [20]. Every value of CQI corresponds to a specific MCS. The data destined to each UE are mapped into modulation symbols according to the MCSs supported by the LTE-A standard, e.g., QPSK and 64-QAM. The MCS chosen for each transmission affects the number of bits carried per symbol.

For MCS selection, the SNR of each eNB-UE link must be

estimated. We consider independent downlink channels with Rayleigh fading. Thus, the SNR is a random variable with average value  $\gamma$  and probability density function given by:

$$f(y) = \frac{1}{\gamma} e^{-\frac{y}{\gamma}} u(y), \quad (1)$$

where  $u(y)$  is the unit step function.

### B. D2D communication

The active UEs ( $UE_1$  and  $UE_2$ ) intend to initiate a bidirectional communication among them (Fig. 1). The packet arrival rate of each active UE depends on the downlink data rate. After the reception of packets, the two UEs contend for Wi-Fi channel access using the Distributed Coordination Function (DCF) of IEEE 802.11 specification [29], which is based on the Carrier Sense Multiple Access with Collision Avoidance (CSMA/CA) method, and attempt to exchange their data.

Erroneous packet transmissions might occur due to fluctuations of D2D links' quality. An active UE that fails to decode a packet asks for cooperation from idle UEs in close proximity that opportunistically overhear the packets exchanged during  $UE_1 \leftrightarrow UE_2$  communication. The neighboring UEs decide whether they will join the relay set  $\mathbf{R} = \{r_1, r_2, \dots, r_N\}$ , depending on their mode (transmission or idle), and whether NC packets can be transmitted during the cooperation.

In channel model, fading is considered using the packet error rate (PER). The ergodicity of the fading process enables the use of bit error probability, which is directly related to PER [30]. The wireless channels between active UEs and relays are assumed to be independent of each other. We denote the PERs in the  $UE_1 \leftrightarrow r_n$  and  $UE_2 \leftrightarrow r_n$  D2D links,  $r_n \in \mathbf{R}$ , as  $PER_{(UE_1 \leftrightarrow r_n)}$  and  $PER_{(UE_2 \leftrightarrow r_n)}$ , respectively.

The retransmissions of the active UE pair's packets by relays imply contention for channel access, resolved by the DCF method that uses various contention windows and backoff stages. A relay ready to transmit selects its backoff counter in a specific contention window range. Each relay may overhear zero, one or two packets of the two active UEs. In bidirectional communication, it is efficient that the relays serve simultaneously packets of both flows. However, the default DCF operation does not favor the selection of the relay with the higher number of overheard packets. ACNC-MAC exploits the NC potential in cooperative D2D transmissions by prioritizing relays capable of performing encoded transmissions.

## III. ADAPTIVE COOPERATIVE NC-BASED MAC (ACNC-MAC) PROTOCOL

In this section, the ACNC-MAC protocol operation is detailed. ACNC-MAC supports the bidirectional communication of active UE pairs. It is compatible with the IEEE 802.11 standard and allows idle UEs within Wi-Fi range to act as relays. It adapts the relays' contention phase to the number of overheard packets, harnessing NC opportunities, and operates as a simple cooperative protocol when NC cannot be performed.

Upon the reception of a packet from the eNB, any of the two UEs can initiate a communication round. Each UE that wishes to transmit contends for channel access by sensing the

channel idle for DCF Inter Frame Space (DIFS) and waits for a random backoff period. The cooperation of adjacent idle UEs is triggered by the transmission of a *Request-for-Cooperation* (RFC) frame, right after a Short Inter Frame Space (SIFS) waiting period. The RFC is sent by the active UE that fails to decode a packet transmitted by the other active UE. If it has a packet of its own to transmit, it is sent piggy-backed with the RFC, which initiates the cooperation phase of ACNC-MAC.

Once other UEs in the area receive the RFC, they decide whether they can act as relays. Each relay candidate receives at most two packets (one from each active UE), thus relays with zero, one or two packets may coexist in the relay set. ACNC-MAC prioritizes the relays with the highest number of overheard packets for the retransmission process, adopting a priority-based backoff counter selection mechanism. Letting  $i$  be the number of packets correctly decoded by a relay and  $cw(k)$  the contention window of the  $k$  DCF backoff stage, each relay selects the backoff value with a contention window  $cw_i \in [cw_{\min}, cw_{\max}]$  as follows:

$$cw_i \in \begin{cases} [2cw(k), 3cw(k) - 1], & \text{if } i = 0 \\ [cw(k), 2cw(k) - 1], & \text{if } i = 1 \\ [0, cw(k) - 1], & \text{if } i = 2 \end{cases} \quad (2)$$

The relay that wins the contention transmits a special control frame, i.e., *Eager-To-Cooperate* (ETC), which indicates the number of packets  $i$  that it is going to transmit (one packet or two packets encoded together). Transmitted after a SIFS period and a priority-based backoff period, ETC informs the two active UEs about the number of ACKs that will terminate the cooperation phase, and deters them from attempting new transmissions before all packets are delivered. It is possible that no ACK frames are transmitted, if none of the exchanged packets has been successfully decoded by any of the relays. Hence, the cooperation ends with the reception of an ETC frame, one ACK frame or two ACK frames by the UE pair.

ACNC-MAC handles three different cases according to the number of packets delivered during the cooperation phase:

*Case 0:* None of the relays have correctly received any packet of the active UE pair (Fig. 2(a)). No ACK frame will be sent and the cooperation ends with the reception of an ETC frame.  $UE_1$  wins the contention phase and transmits its packet  $p_1$ , which is not received by any relay, thus only the ETC frame is sent. In the meanwhile, during the first cooperation round, a packet  $q_1$  has arrived in  $UE_2$ . Afterwards,  $UE_2$  gains channel access and transmits  $q_1$ .  $UE_1$  also has packet  $p_1$ , so it sends RFC piggy-backed with  $p_1$ . The relays fail to receive either  $p_1$  or  $q_1$ , so the cooperation ends with an ETC frame.

*Case 1:* Some relays have received only one packet while others have failed to decode any packet (Fig. 2(b)). The selected relay transmits ETC along with one packet (of either of the two active UEs). ETC indicates that the cooperation phase will terminate by the transmission of only one ACK by the receiver UE. The packet  $p_1$  of  $UE_1$  is received by at least one relay, so the cooperation phase is terminated with the transmission of an ACK frame by  $UE_2$ . A packet  $q_1$  has arrived in the buffer of  $UE_2$ , which wins the contention phase

and sends  $q_1$ .  $UE_1$  fails to decode it and asks for cooperation by sending RFC. As a new packet  $p_2$  has arrived in buffer,  $UE_1$  also sends  $p_2$  along with the RFC. Each relay has at most one packet ( $q_1$  or  $p_2$ ), thus relays with contention windows  $cw_0$  or  $cw_1$  may exist simultaneously. If a relay that has correctly decoded  $q_1$  wins the contention phase, the cooperation ends when  $UE_1$  transmits an ACK frame for  $q_1$ .

**Case 2:** This case occurs only when both UEs have transmitted packets and at least one relay has received them (Fig. 2(c)). The relay that wins the contention phase transmits the ETC piggy-backed with an NC packet. Hence, two ACK frames are expected to end the cooperation phase.  $UE_1$  first sends its packet  $p_1$  and  $UE_2$  transmits its own packet  $q_1$  with the RFC. Relays with zero, one or two packets may coexist and select their backoff periods using the corresponding contention windows  $cw_0$ ,  $cw_1$  and  $cw_2$ . The NC packet is transmitted by the relay that wins the contention phase along with the ETC. At the end of the cooperation phase, both  $UE_1$  and  $UE_2$  confirm the reception of  $q_1$  and  $p_1$ , respectively.

The NC operation is based on the XOR function and the butterfly structure [22]. In Fig. 3(a), the nodes  $S_1$  and  $S_2$  aim to send packets  $a_i$  and  $b_i$  to both  $D_1$  and  $D_2$ , which can overhear the transmission of  $a_i$  and  $b_i$ , respectively. The relay  $R_2$  transmits an encoded packet  $a_i \oplus b_i$ , thus delivering two packets with one transmission and achieving the multicast capacity. By receiving the encoded packet, the destination nodes  $D_1$  and  $D_2$  can obtain the original packets  $b_i$  and  $a_i$ , respectively. In Fig. 3(b),  $UE_1$  and  $UE_2$  are willing to exchange their original packets  $p$  and  $q$ , respectively. The selected relay ( $r_N$  in the example) receives both packets, encodes them using the XOR function and multicasts the encoded packet  $p \oplus q$ , operating in a similar manner as relay  $R_2$  in Fig. 3(a). Using the encoded packet  $p \oplus q$  and its own packet, each UE can decode the original packet, e.g.,  $UE_1$  can decode  $q$ , as it already has its own packet  $p$ .

#### IV. CROSS-NETWORK ANALYSIS OF D2D THROUGHPUT

In this section, we provide a cross-network theoretical model of ACNC-MAC throughput performance, used for D2D data exchange between two UEs that concurrently receive packets from cellular links. The proposed model jointly captures the dynamics of both cellular and D2D connectivity.

The ACNC-MAC cooperation terminates with one of three possible outcomes (ACNC-MAC cases), according to the number of packets originally transmitted (one or two) and the number of packets successfully delivered (up to two). As the duration of each communication round varies analogously, the delay induced by each outcome must be weighted by the corresponding probability. The probability of occurrence of a case consists of two factors: i) the probability that a packet has arrived to either one or both active UEs, i.e., *packet arrival probability*, and ii) the probability that zero, one or two packets are acknowledged at the end of cooperation, i.e., *packet reception probability*. Thus, we formulate the packet arrival and packet reception probabilities for each case.

As ACNC-MAC employs the IEEE 802.11 DCF, the UEs' channel access must be modeled. If the D2D network operates

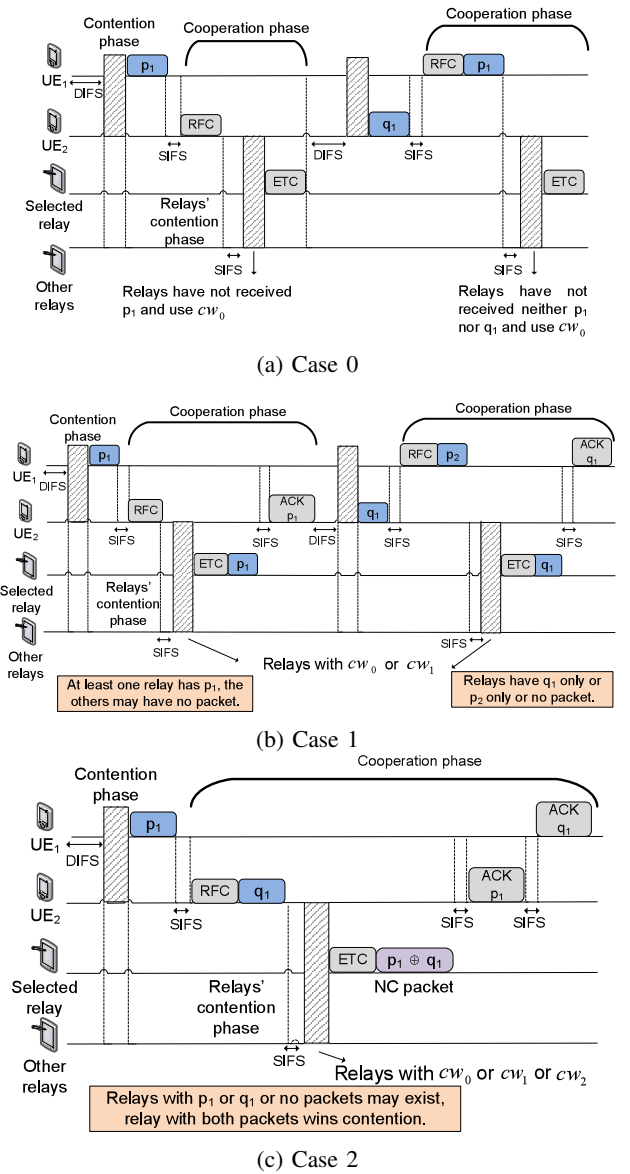


Fig. 2: ACNC-MAC packet sequence for each case

in saturation, i.e., the UEs always have packets to transmit, the bi-dimensional Bianchi model [31] is utilized. It employs a Markov chain to model the backoff window size, used for the estimation of the steady state transmission and collision probabilities required for the throughput estimation. In case of non-saturated conditions, the Malone model [32] is employed, which introduces the idle state in the Markov chain, capturing the event that a UE remains idle between two packet arrivals.

The considered D2D network is formed of two sets of UEs, namely the active UE pair and the set of idle UEs (relays), which operate under different traffic conditions. Actually, the cellular link dependent packet arrival rates impose that an active UE's buffer might be empty, i.e., it operates in non-saturated conditions, hence, for the active UEs backoff counter modeling, we use the Malone model [32]. In contrast to the active UE pair, the set of idle UEs that relay the overheard packets operate in saturated conditions, as they always transmit



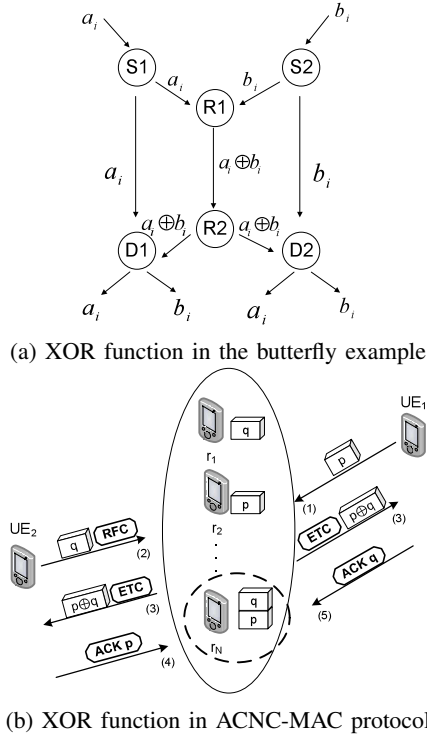


Fig. 3: The XOR function of network coding

at least the ETC frame. All relays participate in the contention phase, but only the relays that have received the most packets are considered to be *active* and may experience collisions. The relays' channel access can be modeled by the Bianchi model [31] using different number of active relays for each ACNC-MAC case. Therefore, it is necessary that the active relay set size per case is analytically derived.

#### A. Packet arrival probabilities

The D2D network operates in conjunction with the cellular network, thus the packet arrival rate is regulated by the eNB that serves the active UEs<sup>1</sup>. The downlink data rate is affected by parameters related to the LTE-A network setup and the wireless channel conditions of the cellular links. The eNB employs a scheduling algorithm that distributes the RBs to UEs. Moreover, the downlink channel state effect is apparent as each UE declares the MCS it supports according to the downlink SNR values. This fact causes variations to the throughput achieved for the UE. The packet arrival rate is affected by the number  $K$  of concurrently active UEs, the number  $N_{RB}$  of available RBs, the packet size  $\ell$ , the packet scheduling policy and the MCS choices. Considering  $S$  different MCSs, the packet arrival rate at a UE is:

$$\lambda = \sum_{i=1}^S \pi_i \frac{L(MCS = i, \lfloor \mathbb{E}[b] \rfloor)}{TTI \cdot \ell}, \quad (3)$$

where the transport block size  $L(MCS = i, \lfloor \mathbb{E}[b] \rfloor)$  can be found in [33]. The expected number  $\mathbb{E}[b]$  of allocated RBs per

UE depends on the scheduling policy. The probability  $\pi_i$  that the  $i$ th MCS is selected is derived as:

$$\pi_i = \int_{\gamma_{thr}^{(i)}}^{\gamma_{thr}^{(i+1)}} f(y) dy = e^{\frac{\gamma_{thr}^{(i+1)}}{\gamma}} - e^{\frac{\gamma_{thr}^{(i)}}{\gamma}}, \quad (4)$$

where  $\gamma$  is the average SNR and  $[\gamma_{thr}^{(i)}, \gamma_{thr}^{(i+1)}]$  is the SNR range that corresponds to MCS  $i$ .

For the throughput analysis, the offered load of the active UE pair can be modeled using the Poisson packet arrival process with mean value  $\lambda$  (packets/s). In our model, we consider two active UEs with corresponding packet arrival rates  $\lambda_1$  and  $\lambda_2$ . Once a packet transmitted by the eNB is received, the UE joins the contention phase following the IEEE 802.11 DCF rules. The two active UEs are not in saturated conditions, as the packets from eNB arrive in variable intervals. For the formulation of probabilities of the ACNC-MAC cases, we consider the probabilities that  $j$  packets arrive at the active UEs. Given that at least one packet is required to initiate the D2D communication, we define the probability  $P(D_j)$ ,  $j \in \{1, 2\}$  that  $j$  packets arrive at the UE pair.

**Lemma 1.** A packet arrives in both UEs with probability:

$$P(D_2) = (1 - e^{-\lambda_1 \mathbb{E}[T_{slot}]}) (1 - e^{-\lambda_2 \mathbb{E}[T_{slot}]}) \quad (5)$$

where  $\mathbb{E}[T_{slot}]$  is the time spent at each state of the Markov chain in the Malone model [32].

*Proof.* The proof of Lemma 1 is provided in Appendix A.  $\square$

**Lemma 2.** Exactly one packet arrives at the D2D network, i.e., only one of the two active UEs receives a packet from the eNB, with probability:

$$P(D_1) = (1 - e^{-\lambda_1 \mathbb{E}[T_{slot}]}) + (1 - e^{-\lambda_2 \mathbb{E}[T_{slot}]}) - (1 - e^{-\lambda_1 \mathbb{E}[T_{slot}]}) (1 - e^{-\lambda_2 \mathbb{E}[T_{slot}]}) \quad (6)$$

*Proof.* When  $D_1$  occurs, a packet arrives at either of the UEs but not in both of them simultaneously. As in Lemma 1, the addition rule is used for the estimation of  $P(D_1)$ .  $\square$

#### B. Packet reception probabilities

The end of cooperation phase is indicated by the reception of i) an ETC frame, if no packet has been successfully received by any relay, ii) a single ACK frame, if at least one relay decodes exactly one packet and no relay has two packets, or iii) two ACK frames, if at least one relay receives packets from both active UEs and performs NC. Each case ensues from the different number of data packets overheard by the  $|\mathbf{R}| = N$  idle UEs. The contingencies of zero ( $C_0$ ), one ( $C_1$ ) or two ACK frames ( $C_2$ ) are mutually exclusive. The contingency  $D_1$  of packet arrival in only one UE and the contingency  $D_2$  of packet arrival in both UEs concurrently form a partition of sample space  $\mathcal{D}$ , as  $D_1 \cap D_2 = \emptyset$  and  $D_1 \cup D_2 = \mathcal{D}$ . Each of the events  $C_i$ ,  $i \in \{0, 1, 2\}$  that form the sample space  $\mathcal{C}$  occur after the packet arrival events  $D_j \in \mathcal{D}$ ,  $j \in \{1, 2\}$ .

**Lemma 3.** If event  $C_i$  occurs after event  $D_j$  with conditional probability  $P(C_i|D_j)$ , the probability that  $C_i$  occurs is:

$$P(C_i) = P(C_i|D_1)P(D_1) + P(C_i|D_2)P(D_2), i \in \{0, 1, 2\}. \quad (7)$$

<sup>1</sup>Our model is also applicable in case that the UEs belong to different cells.

*Proof.* For the events  $D_j \in \mathcal{D}$ , it holds that  $P(D_j) > 0, j \in \{1, 2\}$ . Then, for any event  $C_i, i \in \{0, 1, 2\}$ ,  $P(C_i)$  can be calculated using the total probability formula as  $P(C_i) = \sum_j P(C_i \cap D_j) = \sum_j P(C_i|D_j)P(D_j)$ .  $\square$

We define  $H_{i,j}$  as the event of termination of cooperation with  $i$  ACK frames, i.e., the event that the relays have  $i$  packets, after the transmission of  $j$  packets, and  $P(H_{i,j}) \equiv P(C_i|D_j)$  as its corresponding probability. The duration of each transmission round varies with the number of packets exchanged. Hence, the total time required for the packet(s) successful delivery, or the end of cooperation with ETC frame is weighted using the following probabilistic coefficients:

- (i) *Cooperation ends with ETC frame ( $C_0$ ):* Either one or both UEs transmit a packet. The UE that wins the contention phase transmits its packet and the other UE transmits its own packet (if any) piggy-backed with the RFC frame. This case occurs with probability:

$$P(C_0) = P(H_{0,1})P(D_1) + P(H_{0,2})P(D_2), \quad (8)$$

where

$$P(H_{0,j}) = \prod_{n=1}^N [PER_{(UE_1 \leftrightarrow r_n)} P(D_j)] + \prod_{n=1}^N [PER_{(UE_2 \leftrightarrow r_n)} P(D_j)], j \in \{1, 2\}. \quad (9)$$

This probability corresponds to the case that none of the relays succeeds in receiving any packet from the UE pair.

- (ii) *Cooperation ends with one ACK frame ( $C_1$ ):* One or two packets are sent and the relays receive one of them. If both UEs send a packet, all relays fail to correctly decode both packets. The corresponding probability is:

$$P(C_1) = P(H_{1,1})P(D_1) + P(H_{1,2})P(D_2), \quad (10)$$

where the probability that at least one relay has exactly one packet is:

$$P(H_{1,j}) = 1 - \prod_{n=1}^N (1 - P(H_{1,j}^{(n)})), j \in \{1, 2\}. \quad (11)$$

One or two packets are sent and some relays overhear one packet. If two packets are sent, no relay receives both packets. The probability of reception of exactly one packet by relay  $r_n$  when only one UE has transmitted is:

$$P(H_{1,1}^{(n)}) = (1 - PER_{(UE_1 \leftrightarrow r_n)})P(D_1) + (1 - PER_{(UE_2 \leftrightarrow r_n)})P(D_1), \quad (12)$$

and when both UEs have transmitted packets, it is:

$$P(H_{1,2}^{(n)}) = (PER_{(UE_1 \leftrightarrow r_n)} + PER_{(UE_2 \leftrightarrow r_n)} - 2PER_{(UE_1 \leftrightarrow r_n)}PER_{(UE_2 \leftrightarrow r_n)})P(D_2). \quad (13)$$

- (iii) *Cooperation ends with two ACK frames ( $C_2$ ):* This case might occur when both UEs have transmitted packets and at least one relay receives both of them. Thus, the probability that an NC packet is transmitted is:

$$P(C_2) = P(H_{2,2})P(D_2), \quad (14)$$

with

$$P(H_{2,2}) = 1 - \prod_{n=1}^N (1 - P(H_{2,2}^{(n)})) \quad (15)$$

and

$$P(H_{2,2}^{(n)}) = (1 - PER_{(UE_1 \leftrightarrow r_n)})(1 - PER_{(UE_2 \leftrightarrow r_n)})P(D_2), \quad (16)$$

which is the probability a given relay overhears both packets.

As the duration of cooperation phase depends on the number of transmitted packets by the UE pair and the number of packets overheard by the relays, the aforementioned probabilities are used for the throughput estimation in Section IV-D.

### C. Estimation of the active relay set size

We estimate the number of relays that are active during cooperation. Collisions occur only among relays with the most packets, which gain the highest priority in backoff selection.

**Definition 1.** For each ACNC-MAC case  $i \in \{0, 1, 2\}$ , we define the set of relays whose transmissions may lead to collisions as active relay set  $M_i \subseteq R$  with expected size  $|M_i|$ .

For the estimation of  $|M_i|$ , two probabilistic coefficients must be calculated for each case  $i$ : i) the probability  $P(H_i)$  that at least one relay has received  $i$  packets, and ii) the probability  $P(|M_i| = k)$  that  $k$  relays have received  $i$  packets.

**Lemma 4.** Letting  $k$  be the number of relays that have zero, one or two packets in each ACNC-MAC case respectively, the expected active relay set size  $|M_i|$  is expressed as:

$$|M_i| = \sum_{k=1}^N kP(|M_i| = k), i \in \{0, 1, 2\}, \quad (17)$$

where the probability that  $|M_i| = k$  is given by:

$$P(|M_i| = k) = \binom{N}{k} P(H_i)^k (1 - P(H_i))^{N-k}. \quad (18)$$

*Proof.* The proof of Lemma 4 is provided in Appendix B.  $\square$

### D. Throughput analytical formulation

Having presented the essential components for modeling the throughput performance of ACNC-MAC, we now provide the throughput analysis. For the throughput estimation, the expected duration of a D2D communication round  $\mathbb{E}[T_{i,j}]$ , with  $i \in \{0, 1, 2\}$  and  $j \in \{1, 2\}$  must be derived.

**Lemma 5.** The value of  $\mathbb{E}[T_{i,j}]$  is estimated as follows:

$$\mathbb{E}[T_{i,j}] = \underbrace{\mathbb{E}[T_{slot}^{min}]}_{\mathbb{E}[T_{init}]} + \underbrace{SIFS + T_{ETC}}_{\mathbb{E}[T_{init}]} + \mathbb{E}[r]x_{i,j} + y_{i,j} + \underbrace{\mathbb{E}[r]\mathbb{E}[T_{C_i}]}_{\mathbb{E}[T_{i}^{cont}]} \quad (19)$$

where  $\mathbb{E}[T_{i,j}]$  consists of two components:  $\mathbb{E}[T_{i,j}^{min}]$  is the minimum duration of a contention-free cooperation phase and  $\mathbb{E}[T_i^{cont}]$  is the delay due to the relays' contention.

*Proof.* The proof of Lemma 5 is provided in Appendix C.  $\square$

**Proposition 1.** The expected ACNC-MAC throughput is given by Eq. (20), where  $\mathbb{E}[P]$  is the average correctly received useful bits,  $\mathbb{E}[T_{total}]$  is the average time required for a packet to be delivered to its destination and  $\ell$  the packet payload size.

$$\mathbb{E}[S] = \frac{\overbrace{\ell(P(H_{1,1}) + P(H_{1,2})) + 2\ell P(H_{2,2})}^{\mathbb{E}[P]}}{\underbrace{P(H_{0,1})\mathbb{E}[T_{0,1}] + P(H_{0,2})\mathbb{E}[T_{0,2}] + P(H_{1,1})\mathbb{E}[T_{1,1}] + P(H_{1,2})\mathbb{E}[T_{1,2}] + P(H_{2,2})\mathbb{E}[T_{2,2}]}_{\mathbb{E}[T_{total}]}} \quad (20)$$

The terms  $\mathbb{E}[T_{i,j}]$  given by Eq. (19) and the probabilistic coefficients given by Eqs. (9), (11) and (15) are used for the throughput estimation.  $\mathbb{E}[P]$  is weighted by the probabilities that one or two packets are successfully delivered. The delay values that constitute the average delay term are weighted by the probabilities  $P(H_{i,j})$ ,  $i \in \{0, 1, 2\}$  and  $j \in \{1, 2\}$ , i.e., the probabilities of each of the five possible outcomes inferred by the conjunction of the packet arrival contingencies  $D_1$  and  $D_2$  and the ACNC-MAC cases  $C_0$ ,  $C_1$  and  $C_2$ .

## V. PERFORMANCE EVALUATION

In this section, we evaluate the analytical model and study the ACNC-MAC performance for different downlink packet scheduling policies, MCSs and numbers of active UEs. Moreover, we present the performance results for video transmission scenarios and investigate the influence of different idle UE deployments. We use a C++ integrated simulator that implements the schedulers and applies the ACNC-MAC protocol.

### A. Simulation Setup and Evaluation Metrics

We consider a UE pair (Fig. 1) that receives data from the eNB, which serves a total of  $K$  UEs in the cell. The UEs belong to either of two SNR classes  $m_{high}$  and  $m_{low}$  of high and low SNR, respectively and each class includes  $K/2$  UEs. We set a threshold SNR,  $SNR_{thres}$ , as a bound between the two classes. All UEs that experience SNR values higher than  $SNR_{thres}$  use 64-QAM and belong to the  $m_{high}$  class, while the rest of them use QPSK or 16-QAM and belong to the  $m_{low}$  class. For UEs with the same modulation scheme, different coding rates may be used. The minimum SNR value derived in the simulations corresponds to the lowest SNR threshold for the MCS with the lowest modulation order and coding rate.

In LTE-A transmissions, the Round Robin scheduler is used, unless otherwise stated. In D2D links, we use PER as channel quality indicator, as described in Section II-B.  $N$  relays assist the UE pair's communication and all D2D links experience the same PER<sup>2</sup>. The active UEs have both LTE-A and Wi-Fi

<sup>2</sup>We use a fixed PER, since different PER values affect the performance as expected, without influencing our conclusions.

TABLE I: Simulation parameters

Parameter	Value
Cellular network	
$N_{RB}$	100
Bandwidth	20 MHz
Modulation schemes	QPSK, 16-QAM, 64-QAM
Channel model	Rayleigh fading
SNR classes	low: {QPSK, 16-QAM}, high: {64-QAM}
TTI	1 ms
$P_{Rx}^{LTE-A}$	4 W [34]
D2D network	
Tx rate (Mb/s)	54 (data), 6 (control frames)
Payload size	1500 bytes
ETC	16 bytes
DIFS	50 $\mu$ s
RFC, ACK	14 bytes
PER	0.2
$P_{Rx} = P_{idle}, P_{Tx}$ (mW)	1340, 1900 [35]
UE characteristics	$C_0 = 1300$ mAh, $V_0 = 3.7$ V

interfaces concurrently active. The relays use only the Wi-Fi connection. The active UEs' energy consumption  $E$  is the sum of the average energy consumed during the data reception from the cellular link,  $\mathbb{E}[E_{LTE-A}]$  and the energy consumed in D2D transmissions using ACNC-MAC,  $\mathbb{E}[E_{D2D}]$ . The relays' LTE-A interface is not active and only the energy consumption in Wi-Fi interface is considered, thus we set  $E = \mathbb{E}[E_{D2D}]$ . The simulation parameters are summarized in Table I.

In the simulation scenarios of Sections V-B, V-C1 and V-C2, the UE pair uses ACNC-MAC in order to exchange files of 5 MB size concurrently downloaded through the cellular links. Furthermore, considering the escalating proliferation of multimedia-based mobile applications, we assess the ACNC-MAC performance in video exchange scenarios (Section V-C3), where a video sequence is transmitted by the eNB to the UEs and is further exchanged by the UE pair. The video data are delivered by the eNB in H.264/SVC video compression format [36]. The JSVM 9.19 software [37] is used for the encoding of the "BUS" QCIF video sequence with frame rate 15 frames/sec. The generated packets are transmitted over the LTE-A link and once they are received by the UEs, their transmission with ACNC-MAC is initiated.

The ACNC-MAC performance is evaluated in terms of aggregated D2D network throughput and energy efficiency, i.e., the amount of payload bits exchanged over the total energy consumption (measured in bits/Joule) [38]. The amount of useful bits received is the sum of useful bits received by the final destinations, i.e., the sum of bits of useful data received by the D2D pair. The total energy consumption refers to the energy consumed by the D2D pair and the relays. To gain a better insight on energy consumption, in the simulation scenario of Section V-C3, we estimate the average battery drain  $\Delta C = C_0 - C$  (mAh) [39] of the UE pair and the relays, where  $C_0$  is the initial battery capacity.  $C$  is the expected battery capacity, estimated as  $C = (E_0 - E)/(V_0 \cdot 60^2)$ , where  $V_0$  is the battery voltage,  $E_0 = V_0 \cdot C_0 \cdot 60^2$  is the initial energy and  $E$  is the total energy consumption of each UE in Joules.

### B. Model Validation and Comparison with NCCARQ-MAC

For the throughput analysis validation, we assume a cell with  $K \in \{20, 40, 60, 80\}$  UEs. The idle UEs (relays) are



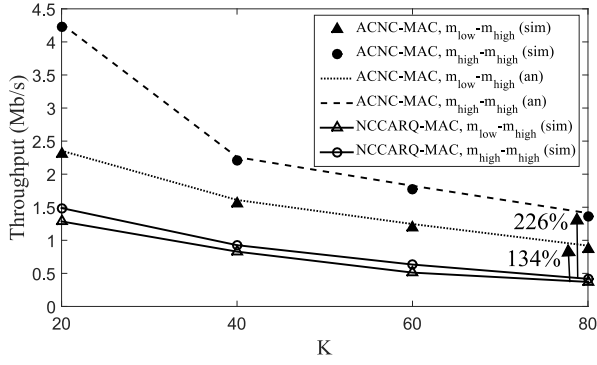


Fig. 4: D2D throughput for different SNR classes vs.  $K$

$N = 5$ . We compare ACNC-MAC with a modified version of NCCARQ-MAC [26] that permits the protocol application in non-saturated conditions incited by D2D communication. With NCCARQ-MAC, the relays cooperate only when they receive packets from both UEs and can perform NC transmissions.

The match of theoretical and simulation results corroborate the throughput analysis (Fig. 4). Moreover, ACNC-MAC outperforms NCCARQ-MAC in terms of throughput, as it exploits more efficiently the cooperation opportunities. The ACNC-MAC throughput is 134% and 226% higher for the  $m_{low-m_{high}}$  and  $m_{high-m_{high}}$  UE pair, respectively ( $K = 80$ ). Notably, when the cell congestion ( $K$ ) increases, both protocols' throughput deteriorates. As more UEs are served in each TTI, fewer RBs are allocated to each UE, reducing the downlink data rate. Thus, the packet arrival rates reduce, increasing the duration of data exchange between the UE pair, as more communication rounds are required to deliver the data. Comparing the ACNC-MAC throughput for  $K = 20$  and  $K = 80$ , we observe a decrease of 62% for  $m_{high}$  UEs and 67% for  $m_{low-m_{high}}$  UEs. However, the ACNC-MAC throughput remains higher than the NCCARQ-MAC throughput. The gain increases along with  $K$ , as packet arrival rates decrease, reducing the NC opportunities. Thus, fewer fruitful communication rounds occur with NCCARQ-MAC.

ACNC-MAC achieves higher energy efficiency than NCCARQ-MAC in all scenarios (Fig. 5). More transmission rounds fail to deliver packets when NCCARQ-MAC is used, whereas ACNC-MAC allows retransmissions by relays, even when only one packet exists in at least one of them. For this reason, ACNC-MAC achieves gains of 34% for an  $m_{low-m_{high}}$  UE pair ( $K = 80$ ), while the gain reaches 38% for the  $m_{high-m_{high}}$  pair. Remarkably, the energy efficiency remains unaffected by the cell congestion levels, as i) longer idle intervals occur, when packet arrival rates decrease, and ii) the energy consumption in idle and reception state is similar.

### C. Impact of LTE-A network deployment on ACNC-MAC performance

In this section, we study the effect of various LTE-A network parameters, i.e., MCSs and downlink packet scheduling policies, on ACNC-MAC performance, and the influence of idle UEs' distributions in a video transmission scenario.

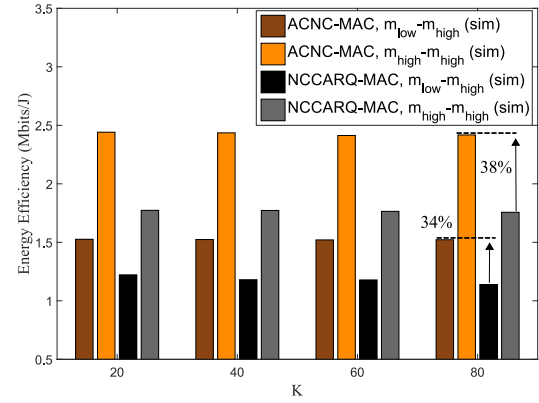


Fig. 5: D2D energy efficiency for different SNR classes vs.  $K$

1) *Effect of MCS choice in downlink transmissions:* Re-visiting Figs. 4 and 5 in Section V-B, we may see that the performance of ACNC-MAC is affected by the MCSs.

The throughput of  $m_{high}$  UEs is significantly better than the throughput of  $m_{low-m_{high}}$  UEs (Fig. 4). With higher order MCSs, the downlink data rates are higher, increasing the packet arrival rates and creating more NC opportunities.

In Fig. 5, we observe that the energy efficiency for the case of  $m_{high}$  UEs is higher than that of  $m_{low-m_{high}}$  UEs. More NC packets are transmitted when UEs with high packet arrival rates communicate. When lower order MCSs are used, relays retransmit only one packet more often and more transmission rounds are required to deliver the same amount of data.

2) *Effect of downlink packet scheduling policy:* Aiming to study the influence of downlink packet scheduling policy on D2D communication performance using ACNC-MAC, we implemented three different scheduling policies, i.e., Round Robin (RR), Maximum Throughput (MT) and Proportional Fair (PF) [19]. The RR scheduler is used as baseline. The MT scheduler maximizes the total throughput of the cell by prioritizing UEs with the best downlink channel SNRs. The PF scheduler aims to find a balance between overall throughput maximization and fairness by concurrently allowing all UEs to receive at least a minimal amount of RBs.

The scheduling policy affects the D2D throughput, although this influence differentiates according to the UEs' SNR class (Fig. 6). Particularly, for the  $m_{high}$  UE pair, the MT achieves higher throughput than the other schedulers, even in high cell congestion, reaching an improvement of 12% ( $K = 60$ ) and 190% ( $K = 80$ ), comparing to PF and RR, respectively. In contrast, for the  $m_{low-m_{high}}$  UE pair, PF improves the throughput, achieving an increase of 24% ( $K = 20$ ) and 43% ( $K = 40$ ), comparing to MT and RR, respectively.

The MT scheduler is favorable for the  $m_{high}$  pair. For the  $m_{low-m_{high}}$  pair, the throughput is higher using PF. This is justified by the way RBs are allocated to UEs. The MT allocates more RBs to the  $m_{high}$  UEs. The prioritization of these UEs in resource allocation induces higher packet arrival rates for them. In contrast, PF treats  $m_{low}$  UEs more fairly. It allocates to them more RBs than MT, thus they experience higher packet arrival rates comparing to the other schedulers.

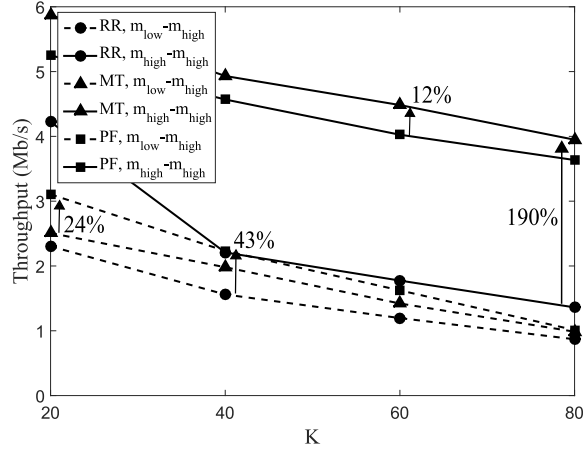
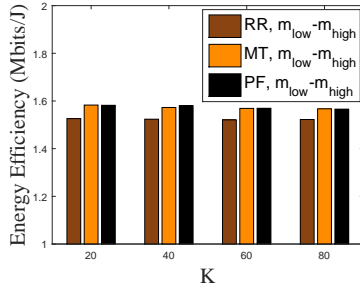
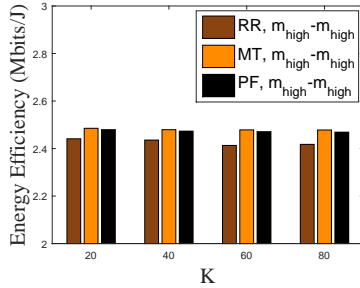


Fig. 6: D2D throughput vs.  $K$  for different downlink packet scheduling policies



(a) Energy efficiency for  $m_{low}$ - $m_{high}$  UE pair

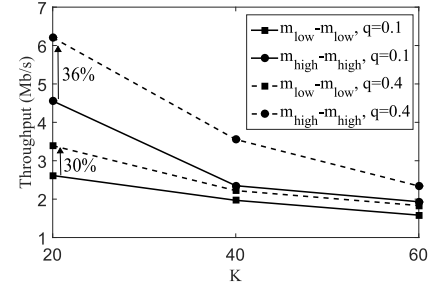


(b) Energy efficiency for  $m_{high}$ - $m_{high}$  UE pair

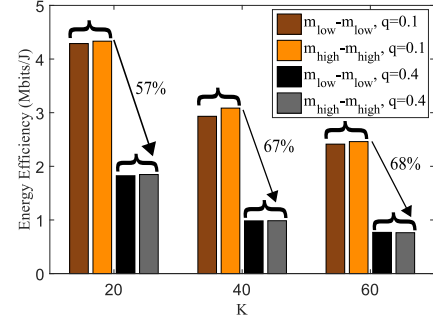
Fig. 7: D2D energy efficiency vs.  $K$  for different downlink packet scheduling policies

Unlike the D2D throughput, different trends are observed in the D2D energy efficiency behavior (Fig. 7). For both UE pairs, all schedulers result in similar energy efficiency. The increase of  $K$  reduces the packet arrival rates, inducing longer idle periods and more unfruitful communication rounds, as packet arrivals become quite scarce. However, the similar energy consumption in idle and reception state leads to similar energy efficiency levels, independently of the scheduling policy and the cell congestion levels.

3) *Effect of different idle UEs-relays proportions:* In the previous scenarios, we set a specific number of idle UEs that perform the cooperative transmissions. In this scenario, we set different proportions of idle UEs (relays). We test ACNC-



(a) D2D throughput vs.  $K$



(b) D2D energy efficiency vs.  $K$

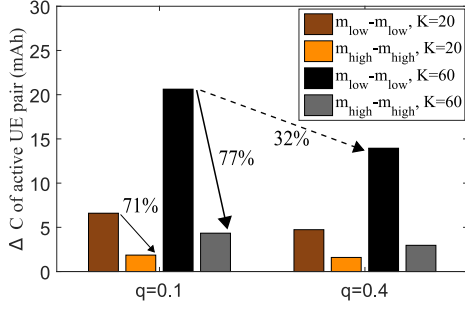
Fig. 8: Impact of different idle UEs proportions on ACNC-MAC throughput and energy efficiency

MAC with number of relays equal to 10% and 40% of  $K \in \{20, 40, 60\}$ , defining their proportion as  $q \in \{0.1, 0.4\}$ .

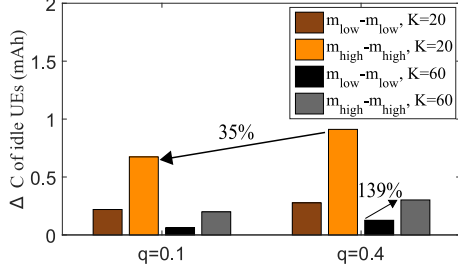
The achieved throughput demonstrates a downward trend as  $K$  increases, independently of the MCS used (Fig. 8(a)). Nonetheless, the throughput of  $m_{high}$  UEs for each  $K$  is higher than the throughput of  $m_{low}$  UEs, which are disfavored even when the number of relays increases. In any case, the throughput performance improves when more relays exist, e.g., comparing the cases of an  $m_{high}$  UE pair and an  $m_{low}$  UE pair ( $K = 20$ ), the throughput is 36% and 30% higher, respectively, when  $q = 0.4$ . This is attributed to the coexistence of fewer active UEs that induces higher data rates and the exploitation of more relays in the ACNC-MAC cooperation phase.

The energy efficiency reduces, when the cell becomes more congested. When more UEs are active, more time is required to deliver the video sequence (Fig. 8(b)). Still, the energy performance for both UE classes is better with  $q = 0.1$ . When more relays are used, the total energy consumption increases. Thus, the energy efficiency is significantly lower, when  $q = 0.4$ . In average, the decrease of energy efficiency reaches 57%, 67% and 68% for  $K = \{20, 40, 60\}$ , respectively. Notably, the increased throughput of scenarios with  $q = 0.4$  does not improve energy efficiency due to relays' high energy consumption.

Additional information about the impact of relays distribution on energy consumption can be derived by the UEs' battery drain levels (Fig. 9(a)). The UE pair's  $\Delta C$  is higher when lower order MCS is used, as the downlink video transmission lasts longer due to lower data rates, e.g., for  $q = 0.1$ , the  $\Delta C$  of an  $m_{high}$  UE pair is 71% ( $K = 20$ ) and 77% ( $K = 60$ ) lower than that of an  $m_{low}$  UE pair, respectively. Equally



(a) Average battery drain of active UE pair



(b) Average battery drain of idle UEs

Fig. 9: Impact of different idle UEs proportions on  $\Delta C$  of UEs using ACNC-MAC

perceptible are the differences between the two idle UEs proportions with regard to the UE pair's energy consumption. In case of an  $m_{low}$  UE pair ( $K = 60$ ), the increase of  $q$  from 0.1 to 0.4 causes a diminution of 32% of the UE pair's  $\Delta C$ . A possible interpretation of this result is that the benefit from the shorter transmission duration when fewer active UEs exist is outweighed by the D2D communication overhead.

In the relays'  $\Delta C$  we observe some different trends from those in the UE pair's  $\Delta C$  (Fig. 9(b)). The relays' battery reduces to a greater extent if the transmissions of  $m_{high}$  UEs are served, e.g., for  $K = 60$  and  $q = 0.4$ , the relays'  $\Delta C$  is 139% higher than the  $\Delta C$  when an  $m_{low}$  UE pair exchanges data. It seems that the throughput improvement of  $m_{high}$  class is accompanied by an increase in relays' energy consumption, as the frequency of packet arrivals is higher and packet retransmissions occur more frequently. Moreover, the relays'  $\Delta C$  is higher when more idle UEs are used, as more relays contend for channel access during the cooperation phase, e.g., in case of an  $m_{high}$  UE pair ( $K = 20$ ), increasing  $q$  leads to 35% higher  $\Delta C$  for the relays.

Overall, the benefit of high order MCSs is depicted on D2D performance, even when the cell congestion increases. However, the scheduling policy influences the D2D performance differently for each UE. UEs with high downlink SNRs experience higher throughput with the MT scheduler, whereas for UEs with poor downlink channel conditions, e.g., in urban environments with obstacles, the PF scheduler is preferable. Moreover, although the use of more relays improves throughput, their number should be properly selected in order to avoid excessive battery consumption that would decrease energy efficiency.

TABLE II: Values of  $x$  and  $y$  terms of Eq. (19)

Case ( $i,j$ )	$x_{i,j}$	$y_{i,j}$
(0,1)	SIFS+ $T_{ETC}$	0
(0,2)	SIFS+ $T_{ETC}$	$T_{pkt}$
(1,1)	SIFS+ $T_{ETC}$	$T_{ACK}$ +SIFS
(1,2)	SIFS+ $T_{ETC}$ + $T_{pkt}$	$T_{pkt}$ + $T_{ACK}$ +SIFS
(2,2)	SIFS+ $T_{ETC}$ + $T_{pkt}^{NC}$	$T_{pkt}$ +2( $T_{ACK}$ +SIFS)

## VI. CONCLUSION

In this paper, a cooperative NC-based MAC protocol (ACNC-MAC) for outband D2D bidirectional communication in LTE-A cell and a throughput analytical model that incorporates characteristics of both LTE-A and D2D links were presented. We assessed the ACNC-MAC performance in the heterogeneous cellular-D2D system under different network setups. ACNC-MAC outperforms the state-of-the-art schemes in terms of throughput. Our work has also shed some light on cellular network-related factors that affect the outband D2D performance and the tradeoffs that arise. The effect of scheduling policies varies with the cellular channel quality, thus each policy is suitable in different cases. The D2D throughput improves when more relays are used, however, the energy efficiency reduces. This may hinder UEs' willingness for cooperation. The cross-network interactions are an attractive topic for future research, as the intricate effects of cellular network characteristics can be investigated in order to organize more effectively the cellular offloading onto D2D connections.

## APPENDIX A PROOF OF LEMMA 1

In ACNC-MAC, a packet arrival to at least one of the two UEs initiates a new transmission round. In a random slot, either of the following events occur: i) no packet arrives at the queue of any UE, ii) a packet arrives at the queue of either of the two UEs, and iii) packets arrive at the queues of both UEs. Thus, a new transmission round will begin when either of the events ii) and iii) occurs. Assuming that packets arrive at a UE  $z$  according to Poisson distribution with rate  $\lambda_z$ , the probability that one or more packets arrive in a time slot is  $P_z = 1 - e^{-\lambda_z \mathbb{E}[T_{slot}]}$  [32]. When the event  $D_2$  occurs, packets arrive at both UEs, thus the probability of packet arrivals  $P(D_2)$  is given by the multiplication rule, as the product of  $(1 - e^{-\lambda_1 \mathbb{E}[T_{slot}]})$  and  $(1 - e^{-\lambda_2 \mathbb{E}[T_{slot}]})$ , which are the probabilities of packet arrival in  $UE_1$  and  $UE_2$ , respectively.

The term  $\mathbb{E}[T_{slot}]$  can be mathematically expressed as [32]:

$$\mathbb{E}[T_{slot}] = (1 - p_{tr})\sigma + 2p_s T_s + p_c T_c, \quad (21)$$

where  $\sigma$  is the idle slot duration, while  $T_s = \text{DIFS} + T_{pkt}$  is the duration of transmission of a packet by a UE and  $T_c = \text{DIFS} + T_{pkt} + \text{SIFS} + T_{RFC}$  is the expected time of collision. The probability that an active UE successfully transmits is  $p_s = 2\tau(1 - \tau)$ , where  $\tau$  is the probability that a UE attempts to transmit in a random slot. The probability that at least one of  $UE_1$  and  $UE_2$  transmits is  $p_{tr}$ , whereas the two UEs experience a collision with probability  $p_c = \tau^2$ . The probabilities  $p_{tr}$ ,  $p_s$  and  $p_c$  are calculated by solving the system of  $\tau$  and the Markov chain's stationary probability at

the initial state,  $b_{0,0}$ . In our case, the probability of having at least one packet to any of the two active UEs utilized by  $\tau$  and  $b_{0,0}$  can be derived as in [32] by setting  $\lambda = (\lambda_1 + \lambda_2)/2$ .

#### APPENDIX B PROOF OF LEMMA 4

At each communication round,  $|M_i|$  out of  $N$  relay candidates contend for channel access and their transmissions may result in collision. The expected value of  $|M_i|$  for each case  $i$  expresses the number of relays that have received  $i$  packets. The probability  $P(H_i)$  of each ACNC-MAC case is:

$$P(H_i) = \sum_{j=1}^2 P(H_{i,j}), i \in \{0, 1, 2\}. \quad (22)$$

As in Section IV-B, we derive the probabilities  $P(H_i) \forall i$ :

- 1) *Case 0*: No relay has received any packet, thus all relays belong to  $M_0$  ( $N = k$ ). Using Eq. (9),  $P(H_0)$  is:

$$P(H_0) = P(H_{0,1}) + P(H_{0,2}). \quad (23)$$

- 2) *Case 1*: Relays with either one packet or zero packets exist. Even if packets from both UEs are transmitted, none of the idle UEs has correctly received both of them. Hence,  $|M_1|$  is equal to the number of relays that have one packet. Using Eq. (11),  $P(H_1)$  is:

$$P(H_1) = P(H_{1,1}) + P(H_{1,2}). \quad (24)$$

- 3) *Case 2*: The active relay set  $M_2$  contains the relays that have received both packets and can perform NC. From Eq. (15),  $P(H_2)$  is:

$$P(H_2) = P(H_{2,2}). \quad (25)$$

Substituting Eqs. (23)-(25) in Eq. (22) yields  $P(H_i), i \in \{0, 1, 2\}$ , required for the estimation of  $P(|M_i| = k)$ .

#### APPENDIX C PROOF OF LEMMA 5

In the first component, i.e.,  $\mathbb{E}[T_{i,j}^{min}]$ , the term  $\mathbb{E}[T_{init}]$  is the delay induced by the initial contention phase between the active UEs. The retransmission duration  $x_{i,j}$ , in case that the relays are perfectly scheduled and collisions do not occur, varies according to the number of retransmitted packets. Similarly, the additional time  $y_{i,j}$  consumed in a contention-free cooperation phase differentiates according to the number of delivered packets, representing the number of ACK frames expected. The values  $x_{i,j}$  and  $y_{i,j}$  are reported in Table II.

The second component, i.e.,  $\mathbb{E}[T_i^{cont}]$ , is the delay caused by the relays' contention, expressed as the product of  $\mathbb{E}[r]$  and  $\mathbb{E}[Tc_i]$ .  $\mathbb{E}[r]$  is the expected number of retransmissions required for the successful reception of all packets by their destinations and is estimated as a function of  $PER_{(UE_1 \leftrightarrow r)}$  and  $PER_{(UE_2 \leftrightarrow r)}$  [40].  $\mathbb{E}[Tc_i]$  is the expected time needed for packets transmissions during the relays' contention.

For the calculation of  $\mathbb{E}[Tc_i]$ , the backoff counter model in [26] is applied. The relays select their backoff times from different ranges dictated by the number of overheard packets. Thus, different values of the average time until a relay

transmits successfully must be considered in correspondence with the ACNC-MAC cases.  $\mathbb{E}[Tc_i] \forall i$  is given by:

$$\mathbb{E}[Tc_i] = \left( \frac{1}{p_i^{suc}} - 1 \right) \cdot \left[ \left( \frac{p_i^{idle}}{1 - p_i^{suc}} \right) \sigma + \left( \frac{p_i^{col}}{1 - p_i^{suc}} \right) T_i^{col} \right], \quad (26)$$

where  $p_i^{suc}$ ,  $p_i^{idle}$ ,  $p_i^{col}$  are the probabilities of having a successful, idle or collided slot [26]. The probabilities utilized by the Bianchi model must be computed separately for each ACNC-MAC case  $C_0$ ,  $C_1$  and  $C_2$  using the respective active relay set size estimations  $|M_0|$ ,  $|M_1|$  and  $|M_2|$ , derived in Section IV-C. Identically, the duration of collision among relays' transmissions  $T_i^{col}$  is different  $\forall i$  and is given by:

$$T_0^{col} = \text{SIFS} + T_{ETC}, \quad (27)$$

$$T_1^{col} = \text{SIFS} + T_{ETC} + T_{pkt}, \quad (28)$$

$$T_2^{col} = \text{SIFS} + T_{ETC} + T_{pkt}^{NC}. \quad (29)$$

#### REFERENCES

- [1] "Cisco Visual Networking Index: Global Mobile Data Traffic Forecast Update, 2014 – 2019," 2015.
- [2] A. Laya, W. Kun, A. Widaa, J. Alonso-Zarate, J. Markendahl, and L. Alonso, "Device-to-Device Communications and Small Cells: Enabling Spectrum Reuse for Dense Networks," *IEEE Wireless Commun.*, vol. 21, no. 4, pp. 98–105, Aug. 2014.
- [3] S. Chen and J. Zhao, "The Requirements, Challenges, and Technologies for 5G of Terrestrial Mobile Telecommunication," *IEEE Commun. Mag.*, vol. 52, no. 5, pp. 36–43, May 2014.
- [4] S. Mumtaz, K.M. Saidul Huq, and J. Rodriguez, "Direct Mobile-to-Mobile Communication: Paradigm for 5G," *IEEE Wireless Commun.*, vol. 21, no. 5, pp. 14–23, Oct. 2014.
- [5] 3rd Generation Partnership Project, "Technical Specification Group Radio Access Network; Study on LTE Device to Device Proximity Services; Radio Aspects (3GPP TR 36.843 version 12.0.1 Release 12)," March 2014.
- [6] J. Liu, N. Kato, J. Ma, and N. Kadowaki, "Device-to-Device Communication in LTE-Advanced Networks: A Survey," *IEEE Commun. Surveys & Tutorials*, vol. 17, no. 4, pp. 1923–1940, 2014.
- [7] "NOKIA White Paper: Optimising Spectrum Utilisation towards 2020," 2014.
- [8] D. Camps-Mur, A. Garcia-Saavedra, and P. Serrano, "Device-to-Device Communications with Wi-Fi Direct: Overview and Experimentation," *IEEE Wireless Commun.*, vol. 20, no. 3, pp. 96–104, June 2013.
- [9] J. Qiao, X. Shen, J. Mark, Q. Shen, Y. He, and L. Lei, "Enabling Device-to-Device Communications in Millimeter-Wave 5G Cellular Networks," *IEEE Commun. Mag.*, vol. 53, no. 1, pp. 209–215, Jan. 2015.
- [10] C. Xu, L. Song, and Z. Han, *Resource Management for Device-to-Device Underlay Communication*, Springer, 2014.
- [11] A. Antonopoulos, E. Kartsakli, and C. Verikoukis, "Game Theoretic D2D Content Dissemination in 4G Cellular Networks," *IEEE Commun. Mag.*, vol. 52, no. 6, pp. 125–132, June 2014.
- [12] A. Asadi, V. Sciancalepore, and V. Mancuso, "On the Efficient Utilization of Radio Resources in Extremely Dense Wireless Networks," *IEEE Commun. Magazine*, vol. 53, no. 1, pp. 126–132, Jan. 2015.
- [13] A. Asadi and V. Mancuso, "On the Compound Impact of Opportunistic Scheduling and D2D Communications in Cellular Networks," in *Proc. ACM International Conference on Modeling, Analysis & Simulation of Wireless and Mobile Systems*, 2013, pp. 279–288.
- [14] Q. Wang and B. Rengarajan, "Recouping Opportunistic Gain in Dense Base Station Layouts through Energy-Aware User Cooperation," in *IEEE WoWMoM*, June 2013, pp. 1–9.
- [15] T. Wang, Y. Sun, L. Song, and Z. Han, "Social Data Offloading in D2D-Enhanced Cellular Networks by Network Formation Games," *IEEE Trans. Wireless Commun.*, vol. 14, no. 12, pp. 7004–7015, Dec. 2015.
- [16] N. Golrezaei, P. Mansourifard, A.F. Molisch, and A.G. Dimakis, "Base-Station Assisted Device-to-Device Communications for High-Throughput Wireless Video Networks," *IEEE Trans. Wireless Commun.*, vol. 13, no. 7, pp. 3665–3676, July 2014.



- [17] M. N. Tehrani, M. Uysal, and H. Yanikomeroglu, "Device-to-Device Communication in 5G Cellular Networks: Challenges, Solutions, and Future Directions," *IEEE Commun. Mag.*, vol. 52, no. 5, pp. 86–92, May 2014.
- [18] Y. Zhang, L. Song, W. Saad, Z. Dawy, and Z. Han, "Contract-Based Incentive Mechanisms for Device-to-Device Communications in Cellular Networks," *IEEE J. Sel. Areas Commun.*, vol. 33, no. 10, pp. 2144–2155, Oct. 2015.
- [19] F. Capozzi, G. Piro, L. A. Grieco, G. Boggia, and P. Camarda, "Down-link Packet Scheduling in LTE Cellular Networks: Key Design Issues and a Survey," *IEEE Commun. Surveys & Tutorials*, vol. 15, no. 2, pp. 678–700, Second 2013.
- [20] 3rd Generation Partnership Project, "LTE; Evolved Universal Terrestrial Radio Access (E-UTRA); Radio Frequency (RF) system scenarios (3GPP TR 36.942 version 12.0.0 Release 12)," Oct. 2014.
- [21] S. Andreev, O. Galinina, A. Pyattaev, K. Johnsson, and Y. Koucheryavy, "Analyzing Assisted Offloading of Cellular User Sessions onto D2D Links in Unlicensed Bands," *IEEE J. Sel. Areas Commun.*, vol. 33, no. 1, pp. 67–80, Jan. 2015.
- [22] R. Ahlswede, C. Ning, S.-Y.R. Li, and R.W. Yeung, "Network Information Flow," *IEEE Trans. Inf. Theory*, vol. 46, no. 4, pp. 1204–1216, July 2000.
- [23] A. Pyattaev, O. Galinina, S. Andreev, M. Katz, and Y. Koucheryavy, "Understanding Practical Limitations of Network Coding for Assisted Proximate Communication," *IEEE J. Sel. Areas Commun.*, vol. 33, no. 2, pp. 156–170, Feb. 2015.
- [24] S. Katti, H. Rahul, W. Hu, D. Katabi, M. Médard, and J. Crowcroft, "XORs in the Air: Practical Wireless Network Coding," *SIGCOMM Comput. Commun. Rev.*, vol. 36, no. 4, pp. 243–254, Aug. 2006.
- [25] J. Zhang, Y. P. Chen, and I. Marsic, "MAC-layer Proactive Mixing for Network Coding in Multi-hop Wireless Networks," *Computer Networks*, vol. 54, no. 2, pp. 196 – 207, 2010.
- [26] A. Antonopoulos, C. Verikoukis, C. Skianis, and Ö. B. Akan, "Energy Efficient Network Coding-based MAC for Cooperative ARQ Wireless Networks," *Ad Hoc Networks*, vol. 11, no. 1, pp. 190 – 200, 2013.
- [27] X. Wang and J. Li, "Network Coding Aware Cooperative MAC Protocol for Wireless Ad Hoc Networks," *IEEE Trans. Parallel and Distributed Systems*, pp. 167–179, Jan. 2014.
- [28] S. Wang, Q. Song, X. Wang, and A. Jamalipour, "Distributed MAC Protocol Supporting Physical-Layer Network Coding," *IEEE Trans. Mobile Computing*, vol. 12, no. 5, pp. 1023–1036, May 2013.
- [29] "IEEE Standard for Inf. technology–Telecommun. and Inf. Exchange between systems, Local and Metropolitan Area Networks–Specific requirements Part 11: Wireless LAN Medium Access Control (MAC) and Physical Layer (PHY) Specifications," *IEEE Std 802.11-2012 (Revision of IEEE Std 802.11-2007)*, pp. 1–2793, March 2012.
- [30] P. Mary, M. Dohler, J.-M. Gorce, G. Villemaud, and M. Arndt, "M-ary Symbol Error Outage over Nakagami-m Fading Channels in Shadowing Environments," *IEEE Trans. Commun.*, vol. 57, no. 10, pp. 2876–2879, 2009.
- [31] G. Bianchi, "Performance Analysis of the IEEE 802.11 Distributed Coordination Function," *IEEE J. Sel. Areas Commun.*, vol. 18, no. 3, pp. 535–547, March 2000.
- [32] D. Malone, K. Duffy, and D. Leith, "Modeling the 802.11 Distributed Coordination Function in Nonsaturated Heterogeneous Conditions," *IEEE/ACM Trans. Networking*, vol. 15, no. 1, pp. 159–172, 2007.
- [33] 3rd Generation Partnership Project, "LTE; Evolved Universal Terrestrial Radio Access (E-UTRA); Physical Layer Procedures (3GPP TR 36.213 version 12.4.0 Release 12)," Dec. 2014.
- [34] A.R. Jensen, M. Lauridsen, P. Mogensen, T.B. Sørensen, and P. Jensen, "LTE UE Power Consumption Model: For System Level Energy and Performance Optimization," in *Proc. IEEE VTC Fall*, Sept. 2012, pp. 1–5.
- [35] J.-P. Ebert, S. Aier, G. Kofahl, A. Becker, B. Burns, and A. Wolisz, "Measurement and Simulation of the Energy Consumption of a WLAN Interface," *Telecommunication Networks Group, Technical University of Berlin*, June 2002.
- [36] H. Schwarz, D. Marpe, and T. Wiegand, "Overview of the Scalable Video Coding Extension of the H.264/AVC Standard," *IEEE Trans. Circuits and Systems for Video Technology*, vol. 17, no. 9, pp. 1103–1120, Sept. 2007.
- [37] ITU-T and ISO/IEC (JVT), "Joint Scalable Video Model 11 (JSVM version 9.19)," March 2011.
- [38] V. Rodoplu and T.H. Meng, "Bits-per-Joule Capacity of Energy-Limited Wireless Networks," *IEEE Trans. Wireless Commun.*, vol. 6, no. 3, March 2007.
- [39] N. Ding, D. Wagner, X. Chen, A. Pathak, Y. C. Hu, and A. Rice, "Characterizing and Modeling the Impact of Wireless Signal Strength on Smartphone Battery Drain," *SIGMETRICS Perform. Eval. Rev.*, vol. 41, no. 1, pp. 29–40, June 2013.
- [40] G. Cocco, D. Gunduz, and C. Ibars, "Throughput Analysis in Asymmetric Two-Way Relay Channel with Random Access," in *Proc. IEEE ICC*, June 2011, pp. 1–6.



**Eftychia Datsika** received her B.Sc. and M.Sc. degree in Computer Science from the Computer Science Department, University of Ioannina, Greece in 2010 and 2012, respectively. She is currently working as an Early Stage Researcher in IQADRAT Informatica S.L., Spain. Her research interests lie in the areas of Long Term Evolution Advanced Networks and Device-to-Device Communication.



**Angelos Antonopoulos** received the Ph.D. degree from the Signal Theory and Communications (TSC) Department of the Technical University of Catalonia (UPC) in 2012. He is currently a Researcher in the SMARTECH department of the Technological Telecommunications Centre of Catalonia (CTTC/CERCA). His main research interests include energy efficient network planning, 5G wireless networks and cooperative communications. He has been nominated as Exemplary Reviewer for the IEEE Communications Letters, while he has received the best paper award in IEEE GLOBECOM 2014, the best demo award in IEEE CAMAD 2014, the 1st prize in the IEEE ComSoc Student Competition (as a Mentor) and the EURACON best student paper award in EuCNC 2016.



**Nizar Zorba** received the B.Sc. degree in electrical engineering from Jordan University of Science and Technology, Irbid, Jordan, in 2002, the M.Sc. degree in data communications and the MBA degree from the University of Zaragoza, Zaragoza, Spain, in 2004 and 2005, respectively, and the Ph.D. degree in signal processing for communications from Universitat Politècnica de Catalunya, Barcelona, Spain, in 2007. He led and participated in over 25 research projects; and authored five patents, two books, seven book chapters, and over 100 peer-reviewed journals and international conferences. His research interests are quality of service/experience, energy efficiency, and resource optimization.



**Christos Verikoukis** got his Ph.D. from UPC in 2000. He is currently a Fellow researcher at CTTC/CERCA and an adjunct associate professor at UB. He has published 105 journal papers and over 170 conference papers. He is a co-author of 4 books, 18 chapters and 2 patents. He has participated in more than 30 competitive projects and has served as the principal investigator of national projects. He has supervised 15 Ph.D. students and 5 postdoctoral researchers. He received a best paper award in IEEE ICC 2011, IEEE GLOBECOM 2014 & 2015, EUCNC/EURACON2016 and the EURASIP 2013 Best Paper Award for the Journal on Advances in Signal Processing. He is currently Chair of the IEEE ComSoc CSIM TC.